The current issue and full text archive of this journal is available at
www.emeraldinsight.com/0961-5539.htm



# Multi-scale computational modelling of flow and heat transfer

Dimitris Drikakis and Nikolaos Asproulis
*Fluid Mechanics and Computational Science Group, Department of Aerospace Sciences, Cranfield University, Cranfield, UK*

Received 9 December 2009
Revised 21 January 2010
Accepted 2 February 2010

## Abstract

**Purpose** – The purpose of this paper is to present different approaches for applying macroscopic boundary conditions in hybrid multiscale modelling.

**Design/methodology/approach** – Molecular dynamics (MD) was employed for the microscopic simulations. The continuum boundary conditions were applied either through rescaling of atomistic velocities or resampling based on velocity distribution functions.

**Findings** – The methods have been tested for various fluid flows with heat transfer scenarios. The selection of the most suitable method is not a trivial task and depends on a number of factors such as accuracy requirements and availability of computational resource.

**Originality/value** – The applicability of the methods has been assessed for liquid and gas flows. Specific parameters that affect their accuracy and efficiency have been identified. The effects of these parameters on the accuracy and efficiency of the simulations are investigated. The study provides knowledge regarding the development and application of boundary conditions in multiscale computational frameworks.

**Keywords** Modelling, Heat transfer, Fluid dynamics, Flow, Microscopy, Gas flow

**Paper type** Research paper

## 1. Introduction

Over the last years, numerical modelling of fluid flow inside micro and nanochannels has drawn the attention of the scientific community primarily due to its effectiveness in assisting the development and optimizing the performance of micro and nano fluidic devices. The nature of the phenomena involved into these devices are dominated by the interfacial interactions due to their high surface-to-volume ratio and are characterized by an inherent multiscale nature (Werder *et al.*, 2005a).

The traditional continuum models tend to neglect the microscopic mechanisms at these scales and therefore cannot entirely represent the flow physics inside micro and nano scale systems (Liu *et al.*, 2007; Priezjev, 2007). In cases where the macroscopic constitutive relations or boundary conditions become inadequate, microscopic models, such as molecular dynamics (MD), have to be employed. Previously, MD simulations have been utilized to study the effect of surface properties, such as nanoroughness and wettability, to the boundary conditions and specifically to the slip generation in the solid-fluid interface (Thompson and Troian, 1997; O'Connel and Thompson, 1990; Priezjev *et al.*, 2005; Yang, 2006; Sofos *et al.*, 2009). The Achilles heel of the molecular simulations is their high computational cost, that restrict their applications to nanoscale systems and time scales below microseconds (Asproluis and Drikakis, 2009). To circumvent the implications arising from the disparity of scales, both spatial and temporal, multiscale frameworks and specifically hybrid atomistic-continuum methods have been developed (O'connell and Thompson, 1995; Delgado-Buscalioni and Coveney, 2003a; Hajiconstantionu, 1999; Kalweit and Drikakis, 2008a; Werder *et al.*, 2005b; Liu *et al.*, 2007; Ren and Weinan, 2005; Schwartzentruber *et al.*, 2007).

International Journal of Numerical Methods for Heat & Fluid Flow
Vol. 20 No. 5, 2010
pp. 517-528

0961-5539
DOI 10.1108/09615531011048222

In the majority of these multiscale frameworks, the molecular description is employed to model a small part of the computational domain where the continuum models fail to capture the physics of the system. The successful application of the hybrid methods is based on the accurate and efficient boundary condition transfer (BCT) between the atomistic and continuum description. The most challenging task is the transfer of macroscopic information on a molecular simulations. The main difficulty is that the microscopic description is associated with more degrees of freedom compared to the macroscopic one and, therefore, given the latter the former cannot be uniquely specified (Hadjiconstantinon, 2005; Kalwict and Drikakis, 2008b).

In this paper, the two main approaches for applying continuum information to a molecular simulation are presented and applied to various scenarios aiming to broaden our understanding to the information transfer across the continuum-atomistic interface.

## 2. Atomistic boundary conditions

MD, which is an atomistic model mainly employed in the multiscale frameworks, is a deterministic method, where the evolution of the molecular system is calculated by computing the particles' trajectories based on the classical molecular model. The governing system of equations for MD is a system of Newton's equation of motion in the form:

$$m_i \ddot{\boldsymbol{r}}_i = -\frac{\partial V_i}{\partial \boldsymbol{r}_i} \tag{1}$$

written for each atom $i$ modelled as a point mass. The potential energy $V_i$ for the atom $i$ is the sum of semi-empirical analytical functions that model the real inter-atomic forces. For the examples employed in the current study, the $6-12$ Lennard-Jones potential is used:

$$V_{ij} = 4 \cdot \epsilon \cdot \left[ \left( \frac{\sigma}{r_{ij}} \right)^{12} - \left( \frac{\sigma}{r_{ij}} \right)^{6} \right], \tag{2}$$

where $r_{ij}$ is the distance between the $i$th and the $j$th particle, $\epsilon$ is the characteristic energy level and $\sigma$ is the molecular length scale defining the position of zero potential energy.

The continuum conditions can be applied to a molecular domain using two different methods. The first one is based on continuous rescaling of atomic velocities (Liu *et al.*, 2007; Nie *et al.*, 2006; Nie *et al.*, 2004; Delgado-Buscalioni and Coveney, 2003a, b; 2004; Fabritiis *et al.*, 2006), and the second one encompasses the application of velocity distribution functions, such as Maxwell-Boltzmann (Hadjiconstanion, 1999; Ren and Weinan, 2005; Hadjiconstantinou and Patera, 1997) or Chapman-Enskog (Garica and Alder, 1998; Schwartzentruber *et al.*, 2008a, b; Wijesinghe *et al.*, 2004; Wijesinghe and Hadjiconstantinou, 2004) distribution.

### *2.1 Rescaling techniques*

Suppose a region $R_{ctr}$ in the molecular domain where the continuum conditions are applied (see Figure 1). In this region, the average velocity of the particles must correspond to the continuum macroscopic velocity $\boldsymbol{u}_{con}$:

$$\frac{1}{M_{ctr}} \sum_{i \in R_{ctr}} m_i \boldsymbol{u}_i = \boldsymbol{u}_{con}, \tag{3}$$

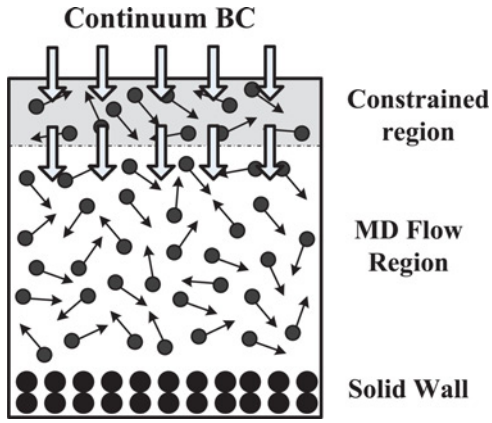


**Figure 1.**
Schematic representation of a molecular region in a hybrid simulation

where $M_{ctr} = \sum m_i,\ i \in R_{ctr}$ is the total mass of particles inside the constrained region. On the basis of Equation (3), the velocities of $\boldsymbol{u}_i$ of the atoms inside the constrained region are periodically replaced by $\boldsymbol{u}'_i$:

$$\boldsymbol{u}'_i = \boldsymbol{u}_i - \frac{1}{M_{ctr}} \sum_{i \in R_{ctr}} m_i \boldsymbol{u}_i + \boldsymbol{u}_{con}. \tag{4}$$

Apart from the velocity restrictions, the continuum pressure should also be applied to the atomistic region. The majority of the hybrid methods usually apply the normal pressure through external forces (Nie *et al.*, 2004; Werder *et al.*, 2005a). In the force-based methods, the application of external forces generates a potential energy field that leads to an energy decrease due to the reduction of the potential energy of the atoms that are moved towards to the continuum boundary. This procedure results in energy oscillations in the molecular system (Kalweit and Drikakis, 2008a, b). One approach that is employed to significantly reduce these oscillations is the velocity reversing of the outermost atoms (Kalweit and Drikakis, 2008a). In this scheme, the continuum pressure, $P_{con}$, is applied by reversing the velocity vector of atoms that move in the opposite direction of the pressure force. If the outer surface of the constrained region is normal to a dimension $\alpha$, then an atom $i$ is reversed by changing the sign of the respective velocity component: $\boldsymbol{v}'_{i,\alpha} = -\boldsymbol{v}'_{i,\alpha}$. For each reversed atom, $i$, a momentum $p_i = 2m_i \boldsymbol{v}'_{i,\alpha}$ is applied. To apply a pressure of $P_{con}$ at each MD time step, the algorithm continues to reverse atoms until the transferred momentum equals the required momentum transfer due to the pressure:

$$\sum_i 2m_i \boldsymbol{v}'_i = P_{con} \Delta t A_{ctr}, \tag{5}$$

where the sum is over the reversed atoms, $\Delta t$ is the size of the time step and $A_{ctr}$ is the surface area of the constrained region. The main advantages of the velocity reversing scheme are simplicity, robustness and the absence of any artifacts due to uncontrolled transfer of energy (Kalweit and Drikakis, 2008a).

The application of the continuum temperature to the molecular system is performed through an energy transfer scheme (Kalweit and Drikakis, 2008a). The main idea is to

add or remove energy from the microscopic system in order to match the macroscopic temperature without modifying the particles' mean velocity. The energy transfer is performed independently for each dimension and is achieved through scaling the velocity vectors of the atoms as follows:

$$\boldsymbol{u}_i' = \boldsymbol{u}_i f + \boldsymbol{c}. \tag{6}$$

The scaling factor, $f$, is calculated by:

$$f = \left(1 + \frac{3N_{ctr}k_B T_{con}}{2E_{k,int}}\right), \tag{7}$$

where $N_{ctr}$ is the number of atoms in the constrained regions, $E_{k,int_a}$ is the internal kinetic energy of these atoms, $k_B$ denotes the Boltzmann constant and $T_{con}$ is the target energy. The internal kinetic energy is given by:

$$E_{k,int} = \sum_{i \in R_{ctr}} \frac{1}{2} m_i (\boldsymbol{u}_i - \bar{\boldsymbol{u}})^2, \tag{8}$$

with $\bar{\boldsymbol{u}}$ being the mean velocity component of the constrained atoms that is calculated by $\bar{\boldsymbol{u}} = (1/M_{ctr}) \sum_{i \in R_{ctr}} m_i \boldsymbol{u}_i$. The factor $\boldsymbol{c}$ is given by:

$$\boldsymbol{c} = \bar{\boldsymbol{u}}(1 - f) \tag{9}$$

and ensures that no momentum is transferred along with the energy.

*2.2 Resampling techniques*

The second BCT method utilizes velocity distribution functions. For the scope of this study, the atomistic velocities are periodically sampled either using the Maxwell-Boltzmann or the Chapman-Enskog distribution. Resampling has been previously applied in MD by other authors in relation to the moving contact line problem (Hadjiconstantinon, 1999; Hadjiconstantinon and Patera, 1997).

The Maxwell-Boltzmann velocity distribution is the natural velocity distribution of an atomic or molecular system in an equilibrium state (Bimalendu, 2002). It defines the probability of the one-dimensional velocity components of an atom assuming a specific value, based on a temperature $T$ and the atom mass $m$.

For the Maxwell-Boltzmann distribution, the probability density $f(\boldsymbol{C})$ of the thermal velocity $\boldsymbol{C} = \boldsymbol{u}/(2k_B T/m)^{1/2}$ is given by:

$$f(\boldsymbol{C}) = \frac{1}{\pi^{3/2}} \exp(-\boldsymbol{C}). \tag{10}$$

Each particle in the BCT region is assigned a velocity $\boldsymbol{u} = \boldsymbol{u}_{continuum} + \boldsymbol{u}_{maxwell}$, where $\mathbf{u}_{maxwell}$ is the velocity of the Maxwellian distribution and $\boldsymbol{u}_{continuum}$ is the macroscopic velocity. The assigned atomistic velocities in the constrained region are then defined as:

$$u_{ia} = u_a^{con} + \sqrt{\frac{k_B T^{con}}{m_i}} \cdot \psi, \tag{11}$$

where $\psi$ denotes a Gaussian distributed number $N(0, 1)$ and $u_a^{con}$ is the $a$th component of the continuum velocity.

In order to ensure that every particle remains inside the molecular domain, a reflective plane is placed at the upper boundary of the BCT region. This is simpler than the velocity reversing scheme, but can only be applied to incompressible flows because the normal pressure is a result of the reflected atoms.

For non-equilibrium situations the Chapman-Enskog distribution is a more appropriate model and, therefore, its application for sampling the atomic velocities has also been investigated. It has been used primarily in hybrid simulations of dilute gases that employ geometrical decomposition and state coupling (Schwartzentruber *et al.*, 2008a, b; Wijsesinghe *et al.*, 2004; Hadjiconstantinou, 2004).

The Chapman-Enskog distribution is a perturbed Maxwell-Boltzmann distribution (Garica and Alder, 1998) with probability density given by:

$$f(\boldsymbol{C}) = \Gamma(\boldsymbol{C})\pi^{-3/2}\exp(-\boldsymbol{C}^2), \tag{12}$$

$\Gamma(\boldsymbol{C})$ is the perturbation term:

$$\begin{aligned}\Gamma(\boldsymbol{C}) = 1 &+ (q_x u_x + q_y u_y + q_z u_z)(\frac{2}{5}\boldsymbol{C}^2 - 1) \\ &- 2(\tau_{x,y}C_xC_y + \tau_{x,z}C_xC_z + \tau_{y,z}C_yC_z) - \tau_{x,x}(C_x^2 - C_z^2) \\ &- \tau_{y,y}(C_y^2 - C_z^2),\end{aligned} \tag{13}$$

where $q_a$ and $\tau_{a,b}$, $a, b = x, y, z$ denote the dimensionless heat flux and stress tensor, respectively. The atomistic velocities for the current distribution are sampled from Equation (12) through the implementation of an acceptance-rejection random velocity generator described in Garica and Alder (1998).

## 3. Results and discussion

### *3.1 Liquid flows*

In the current section, the BCT techniques are applied for liquid heat transfer problems. To quantitatively validate the applied techniques, the outcomes are compared to pure MD simulations. The molecular domain size is 15, 55 and $5\sigma$ in the $x$, $y$ and $z$ directions, respectively. Periodic boundary conditions are applied in the $x$- and $z$-directions. Along the $y$ direction, the domain is constrained by a solid thermal wall from one side and continuum boundary conditions from the other.

In the current simulations, the thermal wall is modelled by two planes of a (111) face-centred cubic (fcc) lattice, where the wall molecules were allowed to vibrate around their lattice sites by a harmonic spring with stiffness $\kappa = 200\,\epsilon/\sigma^2$. The temperature of the wall is maintained through a velocity rescaling algorithm that is applied to each plane separately (Kim *et al.*, 2008). This type of thermal walls operates as heat baths aiming to maintain a thermal equilibrium without the need of an additional thermostat. For the simulations of the current study, the density of the wall atoms and the interaction parameters are $\rho_{wall} = 1.0\,\mathrm{m}\sigma^{-3}$, $\epsilon_{wf} = 0.6\,\epsilon$ and $\sigma_{wf} = 1.0\,\sigma$. These parameters represent a solid wall with no slip boundary conditions (Thompson and Troian, 1997) and correspond to a total number of 136 wall particles. The density of the fluid has been selected to $\rho_{fluid} = 0.8\,\mathrm{m}\sigma^{-3}$ corresponding to the generation of 2,754 particles in the flow and BCT regions. The continuum boundary conditions are applied

in the BCT region which is placed between $45\sigma < y < 55\,\sigma$ and the flow region is between $0\sigma < y < 45\,\sigma$ with height $h$. The simulations are performed for a total $6 \times 10^6$ time steps, with time step $\Delta t_{MD} = 0.001\tau$, and the calculated quantities are averaged over $2 \times 10^6$ time steps.

Initially, the applicability of rescaling method is examined for the a heat transfer problem with $T_{wall} = 1.0\,\epsilon/k_B$, $u_{wall} = 0.5\,\sigma/\tau$ and $T_{con} = 1.03\,\epsilon/\mathrm{k_B}$, $u_{con,x} = 0\,\sigma/\tau$. Two simulations have been performed to study the effect of the BCT region size, in the first one the continuum conditions are applied in the entire BCT region and in the second one the BCT region is divided to four subregions where the continuum state is applied separately to each on of them.

Figure 2 shows the obtained velocity and temperature profiles. It can be identified that the size of the BCT region impacts the consistency of microscopic velocity and temperature with the macroscopic values. In Equation (1), the atomistic velocities are rescaled to a new mean velocity equal to the continuum one. In the current test case, when the continuum information is directly applied to the entire region, the temperature and velocity values in the flow region are slightly underestimated. This inconsistency between the macroscopic and microscopic states introduces inaccuracies in the simulation procedure. To address this issue the BCT region has been further divided to four bins, with height $2.5\sigma$ each, and the macroscopic conditions have been applied to each one of them separately.

For the same temperature and velocity, both for the wall and the BCT region, the rescaling technique and the one based on the Maxwell-Boltzmann distribution are tested. The Chapman-Enskog distribution is utilized when the results obtained from the Maxwell-Boltzmann are not physically correct, typically when the Maxwell-Boltzmann distribution is applied in dilute gases. Pure MD simulations have been performed to provide a point of reference for assessing the validity of the employed techniques. In the pure MD simulations the size of the molecular domain is 15, 90 and $5\sigma$ in the $x$, $y$ and $z$ directions, respectively, and the upper wall is moving with $u_{upper} = -0.5\,\sigma/\tau$ at temperature $T_{upper} = 1.0\ \epsilon/k_B$.

The results from both BCT methods are in good agreement, both between them and with the pure MD simulations, as shown in Figure 3. A linear velocity profile is obtained and the temperature present an increment from $1.0\,\epsilon/k_B$ in the near the wall region to $1.03\,\epsilon/k_B$ near the BCT region.

For a third test case, the continuum conditions applied in the BCT have been $u_{con} = 1.0\,\sigma/\tau$ and $T_{con} = 1.1\,\epsilon/k_B$ and for the pure MD simulation the upper wall is

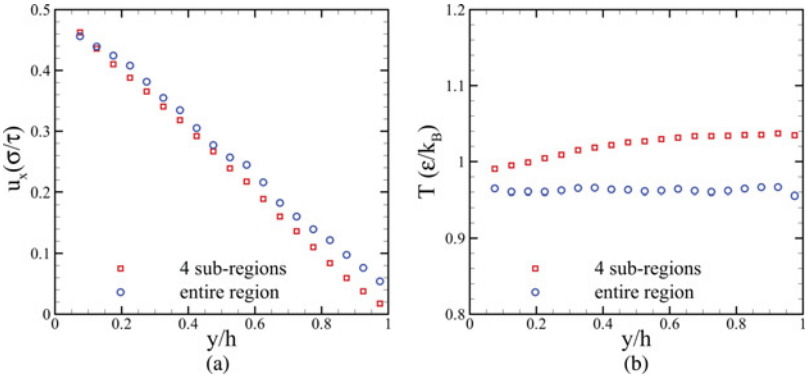


**Figure 2.**
Velocity and temperature profiles with continuum conditions applied to the entire BCT region as well as the BCT region divided into subdomains

moving with $u_{upper} = 1.5\,\sigma/\tau$ at temperature $T_{upper} = 1.2\,\epsilon/k_B$. The results from both techniques are consistent with the molecular outcomes. In Figure 4(a), a small deviation between the resampling and the MD outcomes can be observed mainly caused due to the sampling rate selected for the application of the continuum condition.

*3.2 Gas flows*

The applicability of the BCT methods to gas flows is examined by a second set of test cases. The size of the molecular domain is 200, 120 and 200 $\sigma$ in the $x$, $y$ and $z$ dimensions, respectively, and similar to the liquid flows the domain is divided into two subregions; the flow region located at $y < 100\,\sigma$ and the BCT region at $100\sigma < y < 120\,\sigma$. At the bottom of the molecular domain a stochastic thermal wall is imposed. A stochastic thermal wall is similar to a reflective wall but corrects or resamples the velocity vector of the reflected atom depending on the transferred thermal energy to or from the wall. Such boundary conditions have been extensively used for gas flow simulations (Tenenbaurn, 1983; Tehver *et al.*, 1998; Bhattacharya and Lie, 1991; Xu and Zhou, 2004).

The first test case concerns simulations where the BCT is enforced through a Maxwell-Boltzmann distribution. Three values of density have been simulated $\rho = 0.02\,\mathrm{m}\sigma^{-3}$, $\rho = 0.04\,\mathrm{m}\sigma^{-3}$ and $\rho = 0.08\,\mathrm{m}\sigma^{-3}$ resulting in the generation of 10,240, 20,000 and 40,316 atoms, respectively. The time step used in the MD simulations is $\Delta t_{MD} = 0.001\tau$ and each simulation runs for $8 \times 10^6$ time steps. The macroscopic

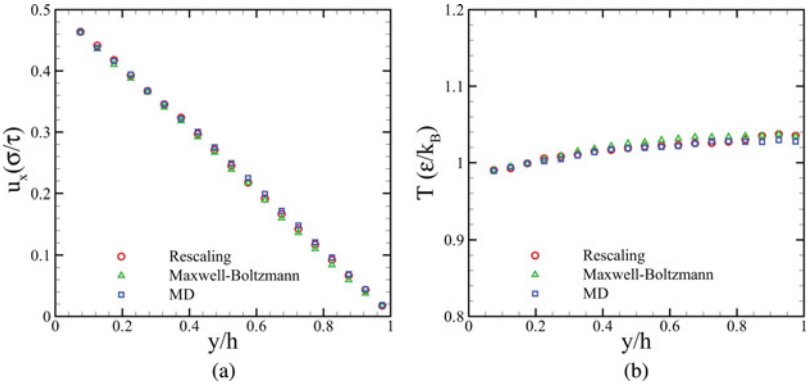


**Figure 3.**
Velocity and temperature profiles with continuum conditions applied to the entire BCT region as well as the BCT region divided into subdomains

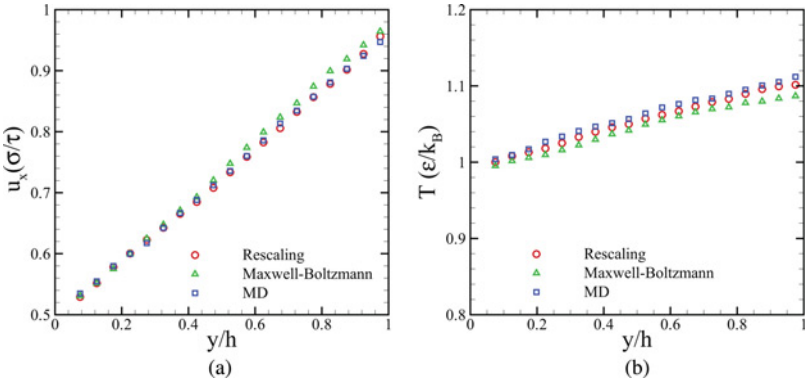


**Figure 4.**
Velocity and temperature profiles with continuum conditions applied to the entire BCT region, as well as the BCT region divided into subdomains

quantities have been averaged over the last $2 \times 10^6$ time steps. The simulations have been performed for different values of gas density with continuum constraints $u_{con,x} = 1.0\,\sigma/\tau$ and $T_{con} = 1.0\,\epsilon/k_B$ and wall temperature $T_{wall} = 1.0\ \epsilon/k_B$.

For low-density gas flows, slip at the boundary is expected, whose magnitude is related to the Knudsen number. High Knudsen numbers result in increased slip (Cao, 2007; Tehver *et al.*, 1998). The Knudsen number is calculated by Bhattacharya and Lie (1991):

$$Kn = \frac{\lambda}{L} = \frac{1}{\sqrt{2}\pi\rho\sigma^2 L}, \tag{14}$$

where $\lambda$ is the mean free path of the gas, $\rho$ is the number density and $L$ is the characteristic length. Equation (14) means that low-density results in higher Knudsen numbers and, consequently, higher magnitudes of the slip velocity. Figure 5(a) shows the velocity profiles obtained from the gas flow using the Maxwell-Boltzmann distribution-based BCT scheme for the three densities. As expected, higher slip velocities near the wall are obtained for lower density values. However, large deviations are observed between the applied velocity constraints and the actual velocity in the upper boundary of the flow region. This is because of an additional slip velocity generated between the flow and BCT regions due to the application of the Maxwell-Boltzmann distribution. Note that lower gas density results in higher deviation between the actual and applied velocity (Wijsesinghe *et al.*, 2004; Hadjiconstantinou and Patera, 1997). To circumvent the unphysical slip at the constrained region, the same simulations have been performed with Maxwell-Boltzmann distribution replaced by the Chapman-Enskog distribution. Figure 5(b) shows velocity profiles obtained with the Chapman-Enskog distribution. Application of this distribution eliminates artificial slip phenomena between the flow and BCT regions.

For the last test case, the rescaling-based technique and the method based on resampling the Chapman-Enskog distribution are utilized for gas flow simulations in the same domain with the previous gas simulations, with density $\rho = 0.05\,\mathrm{m}\sigma^{-3}$, and continuum constraints $u_{con,x} = 1.0\,\sigma/\tau$ and $T_{con} = 1.0\,\epsilon/k_B$ and wall temperature $T_{wall} = 1.0\ \epsilon/k_B$. In the simulations, 25,168 particles have been generated, the MD time step was $\Delta t_{MD} = 0.001\tau$, each simulation was run for $8 \times 10^6$ time steps and the calculated macroscopic quantities were averaged over the last $2 \times 10^6$ time steps.

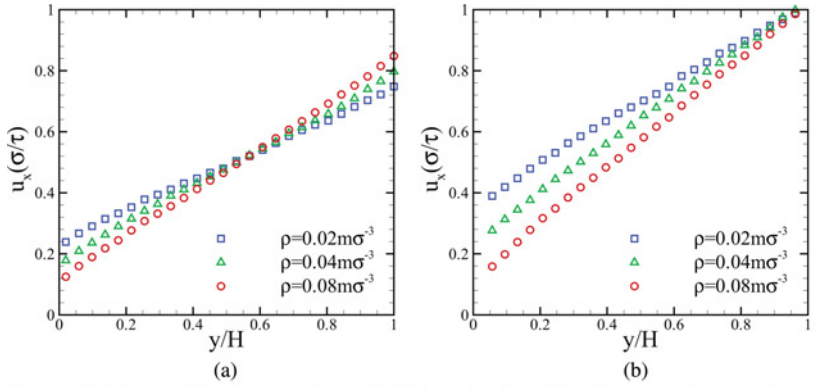


**Notes:** (a) Maxwell-Boltzmann-based BCT method and (b) Chapamn-Enskog-based BCT method

**Figure 5.**
Velocity profiles obtained with Maxwell-Boltzmann and Chapman-Enskog distributions, respectively, for different gas densities

MD simulations of a larger system have been performed to verify the validity of the results. An MD domain of $200\sigma'$ in each direction was selected, comprising a total number of 42,592 particles. The density was $\rho = 0.05\,\mathrm{m}\sigma^{-3}$ and the time step was $0.001\tau$. The simulations have been performed for $8 \times 10^6$ time steps and the calculated quantities have been averaged over the last $2 \times 10^8$ time steps. Two stochastic thermal walls are placed at the upper and lower boundaries of the simulation domain with conditions chosen as $u_{wall,x}^{upper} = 2.0\,\sigma/\tau$, $T_{wall}^{upper} = 0.8\,\epsilon/k_B$ for the upper wall and $u_{wall,x}^{lower} = 0\,\sigma/\tau$, $T_{wall}^{lower} = 1.0\,\epsilon/k_B$ for the lower wall, respectively.

Figure 6(a) shows that results obtained from both BCT methods are in excellent agreement with the large MD simulation. Figure 6(b) shows the velocity distributions for continuum velocity $u_{con,x} = 0.2\,\sigma/\tau = 25\,\mathrm{m/s}$.

## 4. Conclusions

In the present study, various approaches for applying macroscopic boundary conditions to microscopic simulations have been investigated. Specifically, we have drawn attention to the rescaling and resampling BCT schemes and their applicability has been examined under different fluid flow with heat transfer scenarios.

In the rescaling techniques, the molecular domain is constrained not only with the continuum temperature and velocity but also with macroscopic pressure. The application of correct value of pressure is of crucial importance for the accuracy and efficiency of the methods. Inconsistencies in the pressure can shrink the simulation domain or even make particles drift away. This can generate errors and instabilities in the hybrid procedure. Therefore, for the simulations presented here the pressure has been applied through a velocity reversing scheme that presents superior characteristics in terms of stability and accuracy compared to other force-based approaches (Kalweit and Drikakis, 2008a, b). One other parameter that can affect the successful application of these methods and has to be cautiously selected is the size of the regions where the velocity constrains are applied. Inadequate selections can lead to unrealiztic heat transfer across the computational domain and to inconsistencies between the molecular and continuum state.

For the study of the resampling methods, the Maxwell-Boltzmann and Chapman-Enskog distribution function have been employed. The former has been primarily applied to liquid flows and the outcomes have been in good agreement with full

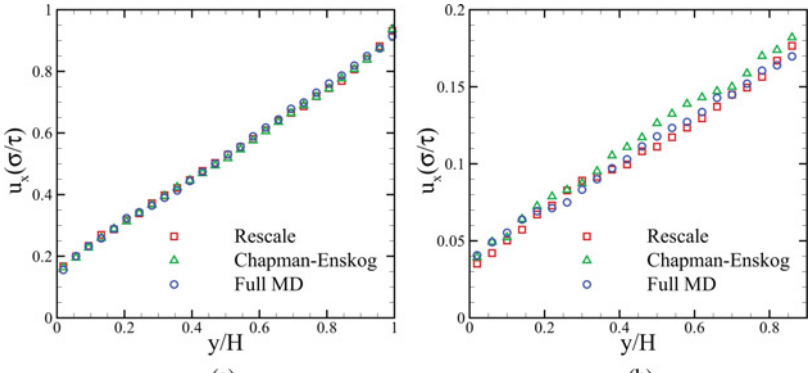


**Notes:** (a) $U_{x-con} = 1\ \sigma/\tau$ and (b) $U_{x-con} = 0.2\ \sigma/\tau$

**Figure 6.**
Velocity profiles for gas with $\rho = 0.05\ \mathrm{m}\,\sigma^{-3}$ obtained from the rescaling BCT method, the BCT method based on the Chapman-Enskog distribution and the full MD simulation

atomistic simulations and with the rescaling BCT method. Two factors that have been identified to have significant impact on the results are the resampling frequency and the termination of the atomistic region. The domain termination is associated with the application of the correct continuum pressure and it is a subject that requires further study. Inadequate sampling frequency can lead to unrealistic effects, such as trapping of particles in the constrained region, or deviations between the macroscopic and microscopic velocities. Selection criteria of these parameters depends on the problem in question and cannot be defined explicitly. The Chapman-Enskog distribution has been applied to circumvent the discrepancies that arose in gas flow simulations when the Maxwell-Boltzmann distribution is applied. The results obtained based on the Chapman-Enskog distribution are in good agreement with full atomistic simulations and the rescaling-based BCT.

Generally, the selection of the boundary transfer scheme is not a trivial issue or a straightforward procedure. It mainly depends on the problem specific parameters along with the available computational resources and the accuracy requirements.

## References

Asproulis, N. and Drikakis, D. (2009), "Nanoscale materials modelling using neural networks", *Journal of Computational and Theoretical Nanoscience*, Vol. 6 No. 3, pp. 514-18.

Bhattacharya, D.K. and Lie, G.C. (1991), "Nonequilibrium gas flow in the transition regime: a molecular-dynamics study", *Physical Review*, Vol. 43 No. 2, pp. 761-67.

Bimalendu, N.R. (2002), *Fundamentals of Classical and Statistical Thermodynamics*, John Wiley, Chichester.

Cao, B.Y. (2007), "Non-maxwell slippage induced by surface roughness for microscale gas flow: a molecular dynamics simulation", *Molecular Physics*, Vol. 105 No. 10, pp. 1403-10.

Delgado-Buscalioni, R. and Coveney, P.V. (2003a), "Continuum-particle hybrid coupling for mass, momentum and energy transfers", *Physical Review E*, Vol. 67, p. 046704.

Delgado-Buscalioni, R. and Coveney, P.V. (2003b), "USHER: an algorithm for particle insertion in dense fluids", *Journal of Chemical Physics*, Vol. 119, pp. 978-87.

Delgado-Buscalioni, R. and Coveney, P. (2004), "Hybrid molecular-continuum fluid dynamics", *Philosophical Transactions of the Royal Society of London A*, Vol. 362, pp. 1639-54.

Fabritiis, G., Delgado-Buscalioni, De, R. and Coveney, P.V. (2006), "Modelling the mesoscale with molecular specificity", *Physical Review Letters*, Vol. 97, p. 134501.

Garcia, A.L. and Alder, B.J. (1998), "Generation of the Chapman-Enskog distribution", *Journal of Computational Physics*, Vol. 140 No. 1, pp. 66-70.

Hadjiconstantinou, N.G. (1999), "Combining atomistic and continuum simulations of contact-line motion", *Physical Review E*, Vol. 59, p. 2475.

Hadjiconstantinou, N.G. (2005), "Discussion of recent developments in hybrid atomistic-continuum methods for multiscale hydrodynamics", *Bulletin of the Polish Academy of Sciences: Technical Sciences*, Vol. 53 No. 4, pp. 335-42.

Hadjiconstantinou, N.G. and Patera, A.T. (1997), "Heterogeneous atomistic-continuum representations for dense fluid systems", *International Journal of Modern Physics*, Vol. 8 No. 4, pp. 967-76.

Kalweit, M. and Drikakis, D. (2008a), "Coupling strategies for hybrid molecularcontinuum simulation methods", *Proceedings of the I MECH E Part C Journal of Mechanical Engineering Science*, Vol. 222, pp. 797-806(10).

Kalweit, M. and Drikakis, D. (2008b), "Multiscale methods for micro/nano flows and materials", *Journal of Computational Theoretical Nano Science*, Vol. 5 No. 9, pp. 1923-38.

Kim, B.H., Beskok, A. and Cagin, T. (2008), "Thermal interactions in nanoscale fluid flow: Molecular dynamics simulations with solid-liquid interfaces", *Microfluidics and Nanofluidics*, Vol. 5 No. 4, pp. 551-59.

Liu, J., Chen, S.V., Nie, X.B. and Robbins, M.O. (2007), "A continuum-atomistic simulation of heat transfer in micro- and nano-flows", *Journal of Computational Physics*, Vol. 227 No. 1, pp. 279-91.

Nie, X.B., Chen, S.Y. and Robbins, M.O. (2004), "A continuum and molecular dynamics hybrid method for micro- and nano-fluid flow", *Journal of Fluid Mechanics*, Vol. 500, pp. 55-64.

Nie, X.B., Robbins, M.O. and Chen, S.Y. (2006), "Resolving singular forces in cavity flow: multiscale modeling from atomic to millimeter scales", *Physical Review Letter*, Vol. 96 No. 13, pp. 1-4.

O'Connel, S.T. and Thompson, P.A. (1990), "Origin of stick-slip motion in boundary lubrication", *Science*, Vol. 250, pp. 792-94.

O'Connell, S.T. and Thompson, P.A. (1995), "Molecular dynamics-continuum hybrid computations: a tool for studying complex fluid flows", *Physical Review E*, Vol. 52 No. 6, pp. R5792-R795.

Priezjev, N.V. (2007), "Effect of surface roughness on rate-dependent slip in simple fluids", *Journal of Chemical Physics*, Vol. 127 No. 14, p. 144708.

Priezjev, N.V., Darhuber, A.A. and Troian, S.M. (2005), "Slip behavior in liquid films on surfaces of patterned wettability: comparison between continuum and molecular dynamics simulations", *Physical Review E*, Vol. 71 No. 4, pp. 041608/1-041608/11.

Ren, W. and Weinan, E. (2005), "Heterogeneous multiscale method for the modeling of complex fluids and micro-fluidics", *Journal of Computational Physics*, Vol. 204 No. 1, pp. 1-26.

Schwartzentruber, T.E., Scalabrin, L.C. and Boyd, I.D. (2007), "A modular particle-continuum numerical method for hypersonic non-equilibrium gas flows", *Journal of Computational Physics*, Vol. 225 No. 1, pp. 1159-74.

Schwartzentruber, T.E., Scalabrin, L.C. and Boyd, I.D. (2008a), "Hybrid particle-continuum simulations of hypersonic flow over a hollow-cylinder-flare geometry", *AIAA Journal*, Vol. 46 No. 8, pp. 2086-95.

Schwartzentruber, T.E., Scalabrin, L.C. and Boyd, I.D. (2008b), "Hybrid particle-continuum simulations of nonequilibrium hypersonic blunt-body flowfields", *Journal of Thermophysics and Heat Transfer*, Vol. 22 No. 1, pp. 29-37.

Sofos, F.D., Karakasidis, T.E. and Liakopoulos, A. (2009), "Effects of wall roughness on flow in nanochannels", *Physical Review E*, Vol. 79 No. 2, pp. 026305/1-026305/7.

Tehver, R., Toigo, F., Koplik, J. and Banavar, J.R. (1998), "Thermal walls in computer simulations", *Physical Review E*, Vol. 57 No. 1, pp. R17-R20.

Tenenbaum, A. (1983), "Local equilibrium in stationary states by molecular dynamics", *Physical Review A*, Vol. 28 No. 5, pp. 3132-33.

Thompson, P.A. and Troian, S.M. (1997), "A general boundary condition for liquid flow at solid surfaces", *Nature*, Vol. 389 No. 6649, pp. 360-62.

Werder, T., Walther, J.H. and Koumoutsakos, P. (2005a), "Hybrid atomistic-continuum method for the simulation of dense fluid flows", *Journal of Computational Physics*, Vol. 205 No. 1, pp. 373-90.

Werder, T., Walther, J. and Koumoutsakos, P. (2005b), "Hybrid atomistic-continuum method for the simulation of dense fluid flows", *Journal of Computational Physics*, Vol. 205, pp. 373-90.

Wijesinghe, H.S. and Hadjiconstantinou, N.G. (2004), "A hybrid atomistic-continuum formulation for unsteady, viscous, incompressible flows", *CMES*, Vol. 5 No. 6, pp. 515-26.

Wijesinghe, H.S., Hornung, R.D., Garcia, A.L. and Hadjiconstantinou, N.G. (2004), "Three-dimensional hybrid continuum-atomistic simulations for multiscale hydrodynamics", *Journal of Fluids and Engineering*, Vol. 126 No. 5, pp. 768-77.

Xu, J.L. and Zhou, Z.Q. (2004), "Molecular dynamics simulation of liquid argon flow at platinum surfaces", *Heat and Mass Transfer*, Vol. 40 No. 11, pp. 859-69.

Yang, S.C. (2006), "Effects of surface roughness and interface wettability on nanoscale flow in a nanochannel", *Microfluidics and Nanofluidics*, Vol. 2 No. 6, pp. 501-11.

**Corresponding author**
Dimitris Drikakis can be contacted at: d.drikakis@cranfield.ac.uk